CLOUD MASK AND TYPES EXTRACTED FROM AVHRR AND GOES IMAGERY

M.Derrien, H.Le Gléau

Météo-France / SCEM / Centre de Météorologie Spatiale
BP 147 22302 Lannion. France

ABSTRACT

This paper presents the automated pixel-scale thresholding techniques being developed at Météo-France to detect and classify clouds from locally-received AVHRR and GOES-8 satellite imageries. The computation of the thresholds, which is the critical part of the method, is detailed [use of atlas and NWP model outputs, precise tuning to AVHRR/GOES spectral characteristics by an off-line use of radiative transfer models (6S, RTTOVS, MODTRAN)]. The accuracy and limits of the method are illustrated using a large test and validation database (interactively fed during one year). Examples of AVHRR cloud types extracted over Europe are presented.

1. INTRODUCTION

Within the SAF in support to Nowcasting and Very Short Range Forecasting (SAF NWC), Météo-France is developing in co-operation with SMHI a software to extract cloud parameters (cloud masks and types, cloud top temperature and height) from MSG SEVIRI imagery over European areas. During the first development phase (1997-1999), prototypes to extract these cloud parameters from locally-received AVHRR imagery (to simulate European conditions) and GOES-8 imagery (to simulate geostationary conditions) are developed in 1998 and will be routinely validated in 1999. The final algorithm tuned to MSG SEVIRI spectral characteristics will be elaborated during a second development phase in 2000, taking advantage of experience gained during the prototyping phase.

This paper focuses on the thresholding techniques being developed at Météo-France to detect and classify clouds from AVHRR and GOES-8 satellite imageries within the SAF NWC project. After having outlined the aim of the AVHRR and GOES prototyping, we give details on the multi-spectral threshold technique itself. In particular, we show how using atlas maps and NWP model outputs allows to apply the method on various regions, and how the precise tuning to AVHRR/GOES spectral characteristics is performed by an off-line use of radiative transfer models. The accuracy and limits of the method are illustrated using a large test and validation database

(interactively fed during more than one year). Examples over Europe (with AVHRR imagery) are presented.

2. AIMS OF AVHRR AND GOES PROTOTYPES

The software, that will be developed within the SAF NWC frame to extract cloud parameters from MSG SEVIRI imagery, should be ready very soon after MSG launch. Therefore, prototypes using AVHRR and GOES-8 imagery locally received at CMS/Lannion are being developed, both to validate algorithms and to check the technical feasibility of real-time processing.

SEVIRI channel	Present Meteosat	GOES-8 imagery	AVHRR/3
VIS 0.6	0.4µm-1.1µm	X	X
VIS 0.8			X
VIS 1.6			X
IR 3.8		X	X
IR 8.7			
IR 10.8	10.5µm-12.5µm	X	X
IR 12		X	X
WV 6.2	5.7µm-7.1µm	6.7µm	
WV 7.3			
IR 9.7			
IR 13.4			
HRV [0.6µm-0.9µm]			

Table 1. Comparison of channel availability on AVHRR, GOES and MSG SEVIRI imagery.

In fact, most of the channels available on MSG SEVIRI and useful for cloud detection and classification are also available both on AVHRR and GOES-8 imagery (see table 1) :

- AVHRR (locally received at Lannion) will allow us to test algorithms in European conditions. We improved and adapted an existing AVHRR processing scheme (Ref.2) to produce cloud categories as close as those defined in the SAF NWC.
- GOES-8 images, which are available every 30 minutes over a large area covering North America and north-west Atlantic Ocean (see figure 1), will simulate geostationary conditions. A completely new scheme is being developed, following specifications defined in the SAF NWC.

The use of radiative transfer model to tune algorithms to the exact channels' spectral characteristics should allow a fast and easy tuning to MSG SEVIRI.

21 identified categories defining the pixel characteristics are listed below. The highest priority is the identification of the major cloud classes, i.e. low, medium, high, semi-transparent. Of secondary importance will be the distinction between convective and stratiform clouds :

-land non contaminated by clouds/aerosol/snow
-sea non contaminated by clouds/aerosol/ice/snow
-land contaminated by snow
-sea contaminated by ice/snow
-very low clouds (2 possible classes : cumuliform and non-cumuliform)
-low clouds (2 possible classes : cumuliform and non-cumuliform)
-medium clouds (2 possible classes : cumuliform and non-cumuliform)
-high opaque clouds (2 possible classes : cumulonimbus and non-cumulonimbus)
-semi-transparent ice clouds (4 possible classes : 3 classes according to thickness + cirrus above clouds)

-fractional clouds
-aerosol (2 possible classes : volcanic/sand)
-unclassified
-non-processed

A “water cloud” flag and a “quality” flag are also parts of the cloud type product.

3. CLOUD MASK AND TYPES THRESHOLDING ALGORITHM

3.1 GENERALITY ON THE METHOD

Pixels are classified in two steps. Clouds are first distinguished from cloud free surfaces during the cloud mask process by a comparison to simulated radiative surface properties. Cloudy pixels are then classified in major cloud classes according to their radiative characteristics. Both steps are performed by thresholding techniques. The distinction between stratiform and cumuliform clouds has not yet been studied.

To meet real-time constraints, the threshold computations that do not require satellite imagery, are performed off-line, in a preparation step prior to the availability of the satellite image. These thresholds are computed on segments (for AVHRR, the segment is a 34*39 AVHRR pixels box centred on HIRS spot; for GOES : the segment size is up to the user (we tested 4*4)). The tests are then applied on-line to full resolution satellite imagery using the thresholds that have been computed off-line at the segment resolution and features computed when having the satellite data.

The justification for pre-computing thresholds on segment is of course time constraints, but also registration errors (mainly for AVHRR) and difficulty to compute thresholds at full resolution imagery (climatological maps, NWP model outputs used to compute thresholds are not available at such fine mesh).

3.2 DETAILS ON THE CLOUD MASK :

3.2.1 Cloud detection tests :

During the cloud detection process, every pixel of a segment go through the same tests sequence governed by its illumination (night and day, night, dawn or sunglint for the sunlit portion of the image) and its geographical location (sea, land, coast) [A distinction between sea and land pixels within a coastal segment is done for GOES]. Each test consists in detecting cloudy pixels by thresholding single channels (11µm brightness temperature, visible reflectance), simple combinations of channels (Sea Surface Temperature (derived from satellite imagery), 11-12µm, 11-3.9µm and 3.9-12µm (nighttime only), 3.9-11µm (daytime only) brightness temperatures differences), combined spatial local variances (of 11µm brightness temperatures, of visible reflectances and even of 11-3.9µm brightness temperatures differences) previously computed on a 3 by 3 window for each pixel of the entire region to process. A snow detection test based on the analysis of the contribution of the solar reflected part of the 3.9 µm measurement is also applied at daytime to sunlit enough pixels.

For AVHRR prototype, the process stops when one test triggers. For GOES prototype, a pixel is considered as cloudy if one test is satisfied, but the process stops only when one test is really successful (i.e., the thresholded value is “far” from the threshold). This leads to assign a quality flag: a cloudy pixel is said poorly classified if no test is really successful.

3.2.2 Thresholds’ computation :

To be efficient, most of the thresholds are based on simulations of the cloud free surface radiative characteristics:

- The use of atlas maps (Land/Sea/Coast atlas, elevation atlas) and climatological atlas (monthly minimum sea surface temperature, monthly mean visible reflectances corrected from atmospheric effects) allows to compute refined thresholds in various surface types. All these maps available at about 10km resolution except the land/sea atlas (full imagery resolution) are remapped to the geostationary projection. Figure 1 shows the SST August climatology used to process GOES-8 imagery.

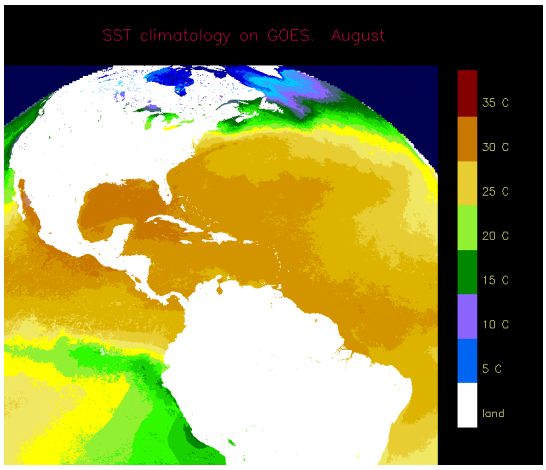

Figure 1. Minimum SST climatology used in the GOES cloud mask.

- NWP outputs (total integrated water vapor content and land ground temperatures) make feasible the adaptation to different atmospheric conditions.
- Finally, radiative transfer algorithms are used to account for satellite geometry and spectral characteristics :
    - for solar channel processing, the radiative transfer model 6S (Ref.[8]) has been applied to pre-compute tables (with angles, water vapor content... as input) that are used together with the bi-directional models developed by Roujean (Ref.[7]) for land and Cox&Munck (Ref.[1]) for sea ;
    - for IR channels thresholding, the radiative transfer model RTTOVS (Ref.3]) has been applied to the TIGR radiosondes dataset (using Masuda tables (Ref.[6]) for sea emissivities) to pre-compute tables (with with angles, water vapor content... as input).

3.2.3 Cloud detection accuracy :

A first estimate of the accuracy and limits of the approach used to compute thresholds has been obtained using a test file (called “interactive test file”). This file contains the geometrical and

radiative characteristics of many small targets (20 000 5x5 pixels for GOES-8 and 6 000 10x10 for AVHRR) manually labelled when selected from numerous images, collocated with their NWP forecast surface and atmospheric parameters, and their atlas extracted informations. These targets are labelled cloud free or contaminated by all sorts of clouds as shown on figure 2.

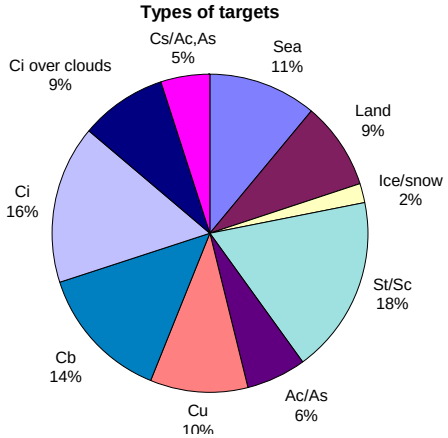

Figure 2. Targets available in the GOES "interactive test file".

For example, the strong bi-directional effects that affect AVHRR visible channel (figure 3a) can be correctly simulated using 6S and Roujean's bi-directional model, especially in the back-scatter direction (figure 3b).

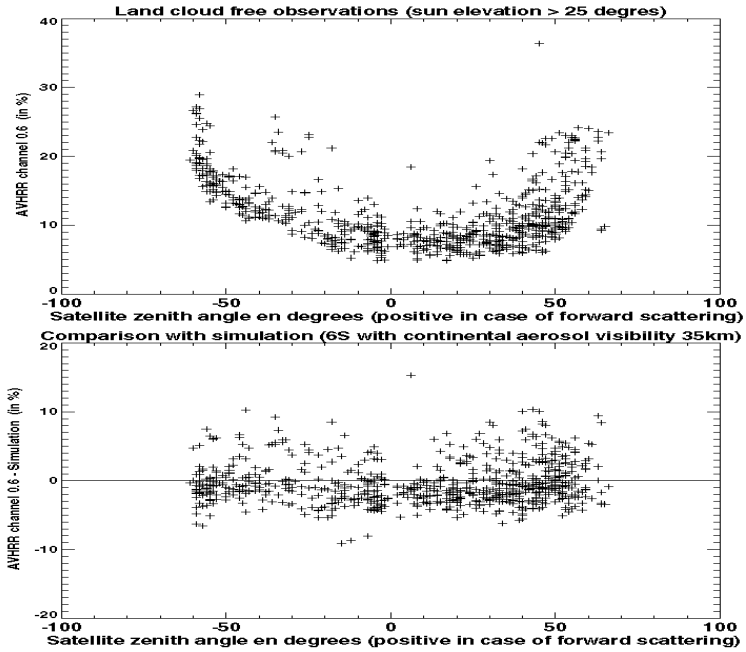

Figure 3. Comparison between AVHRR visible observations and simulations for the "interactive test file" land targets.

The dependency of the 11 and 12 µm brightness temperatures difference over the ocean on the atmospheric water vapor content is illustrated on figure 4a. The threshold deduced from RTTOVS

simulations applied to TIGR radio-sondes data set and the observations of the "interactive test file" presents similar variations, except for very cold seas corresponding to low water vapor content (figure 4b). This remaining effect will be analysed by SMHI as an adaptation to nordic conditions.

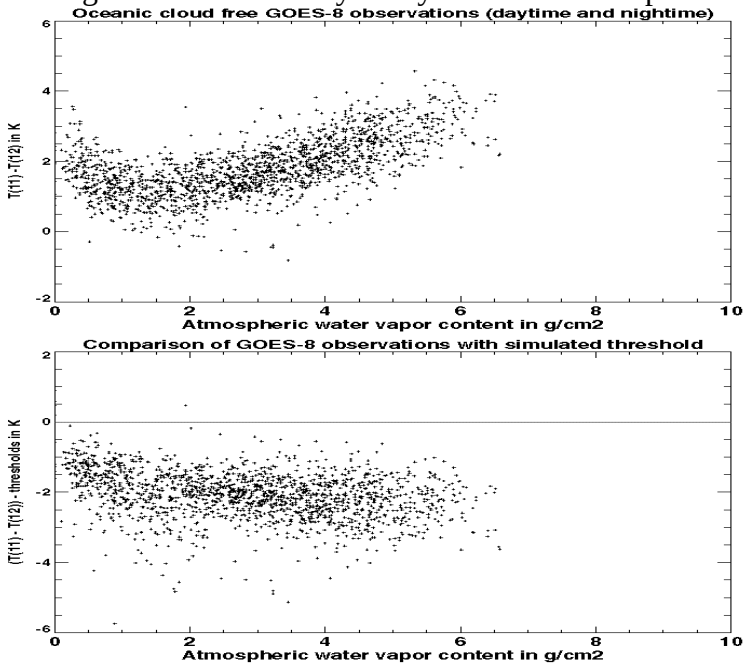

Figure 4. Comparison between observed GOES-8 11 and 12 μm brightness temperatures differences (averaged on a 5 by 5 window to smooth noise) and corresponding simulated threshold for the "interactive test file" cloud free oceanic targets.

Table 2 illustrates the efficiency of the GOES cloud mask in mid-latitude regions (latitudes between 20 and 60 degrees), collated with the "GOES interactive test file" targets. As expected, the quality is slightly better over sea (2.5% targets are mis-classified) than over land (4.4% mis-classified targets). Surprisingly, over sea, results are slightly worse at daytime (3.1%) than at nightime (1.3%) and even at twilight (2.8%, but among fewer cases).

	Cloudy targets correctly detected	Cloudy targets not detected	Cloud free targets mis-classified	Cloud free targets correctly classified
Over sea : day	2380	76	21	701
Over sea : twilight	249	8	0	30
Over sea : night	1333	7	13	206
Over land :day	1679	67	34	578
Over land :twilight	198	11	5	69
Over land :night	533	14	19	226

Table 2. Statistics on the cloud detection algorithm accuracy in mid-latitude regions. Computed on the "GOES interactive file".

3.3 DETAILS ON THE CLOUD TYPES :

3.3.1 Cloud classification tests :

At present time, a sequence of thresholding tests (depending on illumination) is applied to every cloudy pixel to identify the major cloud classes. Neither the distinction between stratiform and cumuliform clouds nor the detection of aerosols is yet performed.

The method can be summarised as stated below :

- The transparent or sub-pixel clouds are distinguished using brightness temperatures differences (11-12 μm for cold pixels or both 11-12 μm and 3.9-11 μm (at nighttime only) but for sufficiently warm pixels to avoid high noise in 3.9 μm). At daytime they are detected by analysing simultaneously visible reflectance and 11 μm infrared brightness temperature. The warmest pixels are supposed to be partly cloudy, whereas when the temperature decreases three cirrus classes are defined according to their 11 μm brightness temperature. At daytime, too high reflectances indicate low or medium clouds beneath the cirrus layer.
- For the other clouds, the separation between low, medium or high clouds is performed by comparing their 11 μm brightness temperature to combinations of forecast atmospheric air temperatures at various levels, such as 700 hPa and 500 hPa for medium clouds for instance. For GOES prototype the levels are selected according to the efficiency of their combinations to regress the separation of the classes of the "interactive test file"

3.3.2 Thresholds' computation :

The thresholds used in the tests described in 3.3.1 are more or less complicated. For example, forecast air temperatures at 700 and 500 hPa are used to separate low, medium and high level clouds, and to define three cirrus classes according to their thickness. The test applied to the visible reflectance to separate semi-transparent from opaque clouds accounts for bi-directional effects over clouds (especially strong on AVHRR and well simulated with Manalo-Smith's model (Ref.[5]), as shown on figure 5) as well as for the surface reflectance beneath the cloud. The 11-12 μm and 3.9-11μm thresholds used to distinguish semi-transparent clouds relies on look-up tables governed by satellite angle and water vapor content. Other ones, such as the threshold applied to local variance on visible channel at daytime to separate cirrus from cumulus are simple parameters. These thresholds are pre-computed before satellite data availability.

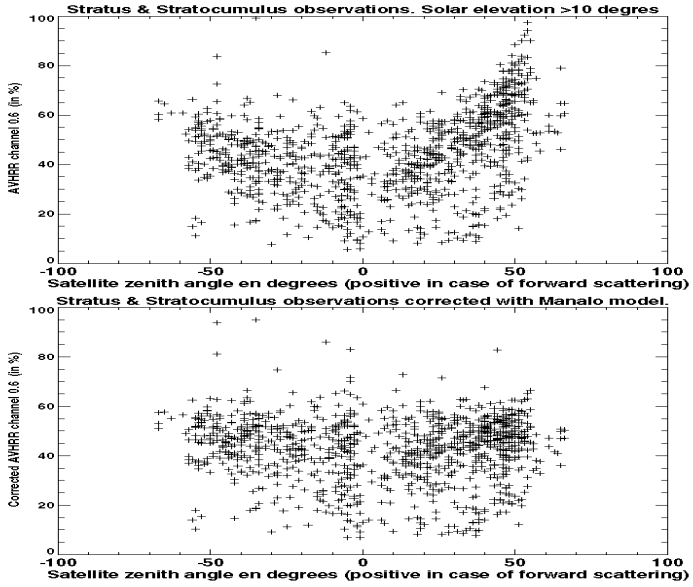

Figure 5. Bi-directional effects in cloud visible reflectances.

3.3.3 Cloud types accuracy :

No statistics have yet been derived on the cloud classification accuracy using the "interactive GOES file", as was done for the GOES cloud mask (3.2.3).

4. EXAMPLES OF AVHRR CLOUD TYPES MAPS

Although the GOES cloud types has been studied in details using the interactive test file, only the GOES cloud mask step has been fully implemented. Therefore, no GOES results are presented in this text.

The AVHRR cloud types maps (upgraded in the SAF NWC context) are routinely computed over the entire AVHRR passes (from north Africa up to Scandinavian countries) that are received at CMS. An area covering France (see figures 6 and 7) is then extracted, remapped onto a polar stereographic grid (at 3km spatial resolution) and sent to all the french forecasters to be displayed either on Meteotel or SYNERGIE workstation.

The two following AVHRR cloud types maps illustrate their usefulness to depict following important phenomena in the area of nowcasting and very short range forecasting :

convective patterns within the unstable air masses (figure 6),
clouds and fog within the atmospheric boundary layer (figure 7).

5. NEXT DEVELOPMENTS :

The algorithm, that has been described in this paper, will be adapted to nordic conditions by the SMHI. It is then planned to go through a validation and tuning period in 1999 ; during this period, the cloud masks and types extracted from the satellite AVHRR and GOES imagery will be visualized (especially during the SAF NWC demonstration phase), and will be routinely compared to cloud observations extracted from SYNOP done by meteorologists from weather ground stations (scattered in America and in Europe), and by sea-based observers from ships.

In 1999, a separation between stratiform and cumuliform clouds using simple thresholding techniques applied to textural features will be attempted. Moreover, the aerosol detection will be developed, using an enlarged "interactive test file" that is presently being gathered. The potentiality of the 1.6 μm channel for water and ice clouds distinction will be studied using the NOAA-15 data collected this summer and those planned to be available in february 1999.

The final algorithm tuned to MSG SEVIRI spectral characteristics will be elaborated during development phase 2 in 2000, taking advantage of experience gained during the prototyping phase.

6. REFERENCES

[1] Cox.C and Munck W, 1954, Measurements of the roughness of the sea surface from the sun's glitter. *J.Opt.Soc.Am*, 44, 838-850.

[2] Derrien M, Farki B., Harang L., Le Gléau H., Noyalet A., Pochic D., A.Sairouni, 1993, Automatic cloud detection applied to NOAA-11 / AVHRR imagery, *Remote Sensing of Environment*, 46, pp 246-267.

[3] Eyre J., 1991, A fast radiative transfer model for satellite soundings systems. ECMWF Res.Dep.Tech.Mem 176. ECMWF, Reading, United Kingdom.

[4] Karlsson K.G., 1996, Cloud classifications with SCANDIA model. SMHI reports Meteorology and Climatology, No 67 (36pps).

[5] Manalo-Smith N., Smith G.L., 1996, Analytic forms of bi-directional reflectance functions for earth radiation budget studies. International Geoscience and Remote Sensing Symposium, Lincoln (USA) 27-31 may 1996.

[6] Masuda K., Takashima T., Takayama Y., 1988, Emissivity of Pure and Sea Waters for the model sea surface in the infrared window regions. *Remote Sensing of Environment* 24 : 313-329.

[7] Roujean J.L., LeRoy M.J., Deschamps P.Y., 1992, A bi-directional reflectance model of the Earth's surface for the correction of remote sensing data. *J.Geophys.res*., 97, 20455-20468.

[8] Tanre D, Deroo C., Duhaut P., Herman M., Morcrette J.J., Perbos J., Deschamps P.Y., 1990, Description of a computer code to simulate the satellite signal in the solar spectrum. *International Journal of Remote Sensing*, 11, pp 659-668.

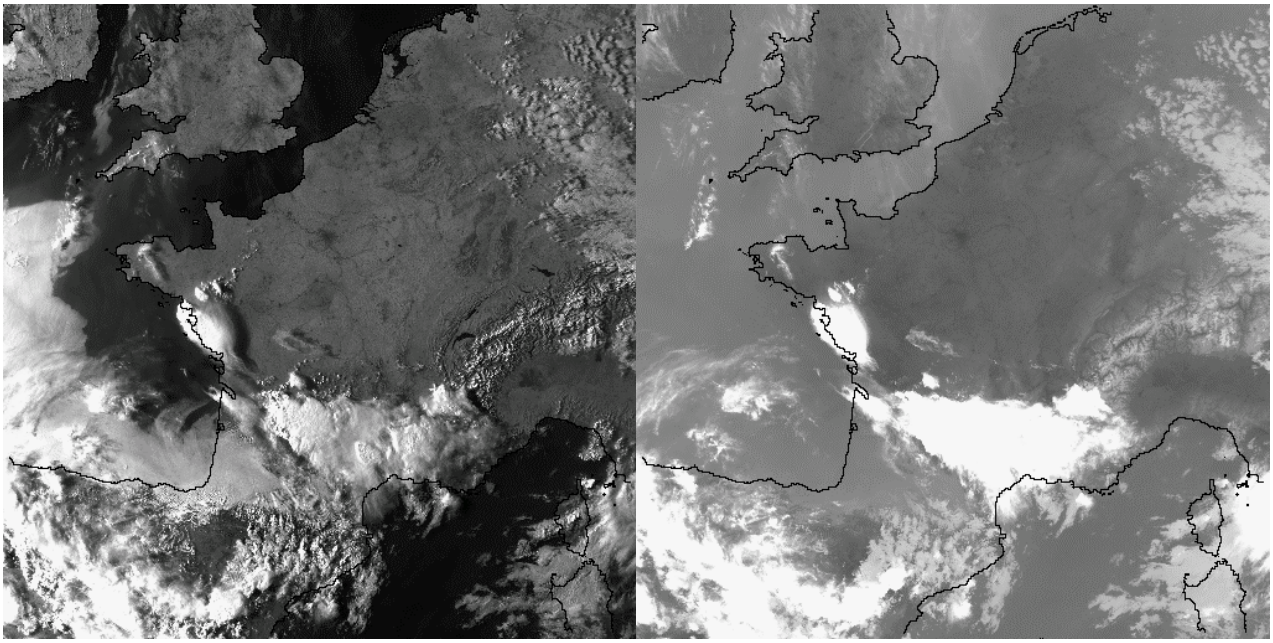

Figure 6a. AVHRR 0.9 µm reflectance (left) and 11 µm brightness temperature (right). NOAA-12 15th May 1998. 17h23 TU

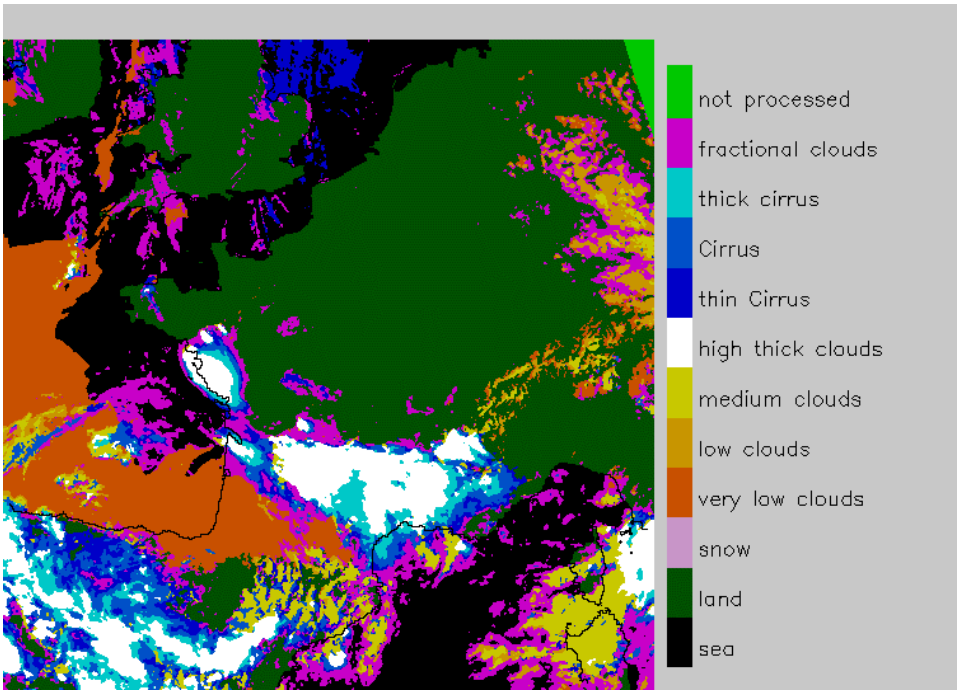

Figure 6b. AVHRR cloud types map. NOAA-12 15th May 1998. 17h23 TU

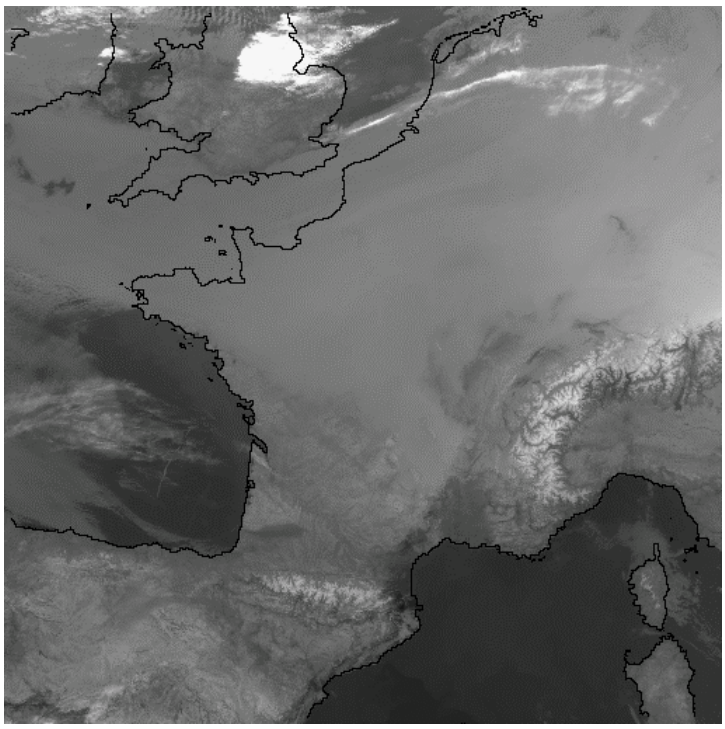

Figure 7a. AVHRR 11 μm brightness temperature. NOAA-14 18th March 1998. 03h11 TU

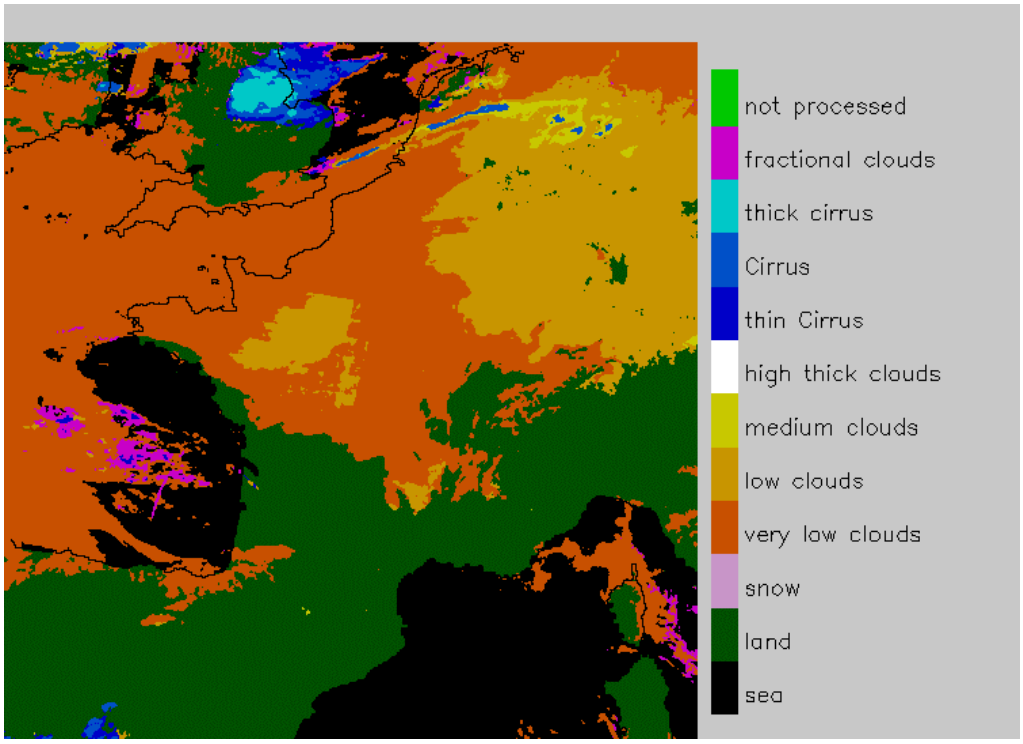

Figure 7b. AVHRR cloud types map. NOAA-14 18th March 1998. 03h11 TU